EurJOC
European Journal of Organic Chemistry

Review
doi.org/10.1002/ejoc.202300070

Chemistry Europe
European Chemical Societies Publishing

www.eurjoc.org

VIP *Very Important Paper*

Special Collection

Photoacidity of Indolinospirobenzopyrans in Water

Cesare Berton[a] and Cristian Pezzato+*[a, b]

The reversible isomerism of indolinospirobenzopyrans is perhaps among the most studied phenomena in the field of molecular switches. Although they began to gain attention as early as 70 years ago following the seminal work of Hirshberg and Fischer, who were the first to recognize their photochromic behaviours, their implementation as photoacids emerged prominently only in the last decade. In this Review, we contextualize the prerequisites underlying the photo-triggered proton release that occurs in these molecular switches, highlighting the most recent advances in their characterization and application as "metastable-state photoacids" in water.

1. Background

Spiropyran compounds are one of the most studied families of molecular switches owing to their ease of synthesis and multifaceted applications.[1–2] Nowadays, the skeletal formula commonly associated with spiropyran molecular switches is the so-called "indoline-pyran" hybrid[3] (abbreviated by IUPAC with the acronym "BIPS"[4]), which results from the condensation of Fischer's bases with salicylaldehydes. The first BIPS was introduced in 1940 by Wizinger and Wenning[5] to elucidate the temperature-dependent intramolecular ionization of spiro compounds and began to be popularized in 1952 by Hirshberg and Fischer[6–10] following the discovery of its photochromic properties.[11] BIPS derivatives are typically composed of a 1,3,3-trimethyl indoline moiety sharing the tetrahedral carbon atom in position 2 with a benzopyran (or chromene) moiety (Figure 1).[12] They exist in a closed-ring spiro form (SP) and an open-ring merocyanine form (MC). The former is colourless, since the two halves of the molecule are located orthogonally to each other via the spiro carbon and therefore are not conjugated, whereas the latter is coloured because the indoline and the chromene parts are coplanar and conjugated through the central ethylene bridge.[13] Interconversion between these two forms can occur with a variety of external stimuli[14] such as light (photochromism), temperature (thermochromism[15]), solvent polarity (solvatochromism[16]), acids (acidochromism[17]), metal ions (ionochromomism[18]), redox potential (electrochromism[19]), and even mechanical stress (mechanochromism[20]). The photochromism can be of two types (Figure 1a). When the thermodynamically most stable state is the colourless SP form, photoexcitation with UV light (<400 nm),H which cleaves the spiro carbon-oxygen bond,[13] results in the formation of the coloured MC form—*i.e.*, the system displays "positive" photochromism. On the other hand, when the thermodynamically most stable state is the coloured MC form, photoexcitation with visible light (>400 nm) triggers a ring-closing reaction leading to the colourless SP form—*i.e.*, the system displays "negative"[21] photochromism.

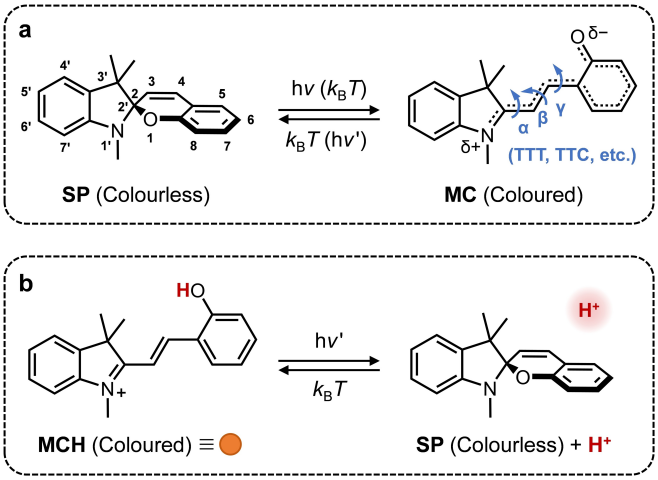

Figure 1. Simplified representation of a) the positive (negative) photochromism of indolinospirobenzopyrans and b) their light-triggered proton dissociation in water; ν and ν' refer to UV and visible light, respectively. Substituents and specific configurations are omitted to bring out the correlation of each species with the proton. It should be noted, however, that SP isomers are chiral species and thus exist in two enantiomeric forms. On the other hand, each of the three bonds separating the indoline and the chromene moieties in the open MC(H) isomers may rotate (thermally or photochemically) around the angles α, β and γ assuming either a *trans* or a *cis* configuration with the respect to the central double bond; in principle, eight different isomeric forms are possible, but only two (TTT and TTC) are known to be stable.[22–25] These considerations hold also for the mechanistic investigations highlighted in Figure 3. In the following figures, an orange circle will be used to represent BIPS in their open protonated form, MCH.

[a] *C. Berton, Dr. C. Pezzato+*
Institut des Sciences et Ingénierie Chimiques
École Polytechnique Fédérale de Lausanne (EPFL)
1015 Lausanne (Switzerland)
[b] *Dr. C. Pezzato+*
Laboratory for Macromolecular and Organic Chemistry (MOC)
Department of Chemical Sciences, University of Padua
Via Marzolo 1, 35131 Padua (Italy)
E-mail: cristian.pezzato@unipd.it

[+] *Cristian Pezzato was nominated to be part of this collection by EurJOC Board Member Maria Valeria D'Auria.*

Special Collection *Part of the "#NextGenOrgChem" and "DCO-SCI Prize and Medal Winners 2020/2021" Special Collections.*

The thermodynamic stability of MC and SP, and therefore the resulting photochromic behaviour, strongly depends on the molecular structure and the solvent polarity.[26–27] Positive photochromism is common with "activated" derivatives (*e.g.*, 6-nitro BIPS) and/or in nonpolar solvents, whereas negative photochromism is mainly observed with "non-activated"[28–29] ones and/or in polar solvents.[30] These photochromic phenomena has been extensively studied over the years, but mostly in organic solvent mixtures and materials.[31] In polar solvents, though, population of the protonated state of MC (MCH) is also possible.[32–33] The aqueous equilibrium of BIPS derivatives in the ground state depends on the pH of the solution and, when it is shifted in favour of MCH, irradiation with visible light can lead to the formation of SP and the concomitant dissociation of a proton (Figure 1b). Eventually, if the dark equilibrium is shifted in favour of SP, irradiation with UV light may lead to ring-opening accompanied by proton uptake.[34–35] In this Review, we will focus only on the first scenario—*i.e.*, only on photoinduced proton transfer phenomena[36] in water. We suggest the readers interested in other physicochemical properties and applications to consult other more comprehensive reviews.[3,31,37–41]

1.1. In quest of persistent and reversible photoacids

Chemical reactions driving predictable pH changes in aqueous solutions can provide easy access to the control of pH-sensitive (bio)chemical systems.[42–43] The growing interest in the development of photoacids—which, in a broad sense, can be defined to as chemical species converting into stronger acids following light absorption—arises from the opportunity to trigger such type of reactions selectively, with high spatial and temporal precision, and without the generation of waste products using light as reactant.[44] Depending on their mechanism of action, photoacids can be classified into three different types, which are: i) photoacid generators,[45] ii) excited-state photoacids,[46] and iii) metastable-state photoacids.[47] Photoacid generators are compounds that produce acids upon photolysis. Typical examples include ionic compounds such as aryldiazonium, diaryliodonium and triarylsulfonium salts or non-ionic compounds such as benzyl esters and sulfones, to name a few; their actuation is generally irreversible and found applications in cationic photopolymerizations and photolithography.[48–49] Excited-state photoacids are compounds displaying extreme acidity differences between their ground state and excited state (the ΔpK_a is comprised from 6 to 13 units[50]). Prominent examples are phenols,[50] naphthols[51] and the pyranine dye, HPTS.[52] Their actuation is reversible, but proton recombination is so fast that modest pH changes are difficult to be observed even using intense light sources.[53] On the contrary, metastable-state photoacids are compounds which, after photoexcitation with light of moderate intensity, can access a dissociated state that is relatively long-lived.[54] They are also fully reversible, as in the absence of light they spontaneously revert to their original less acidic state. Important examples include *ortho*-hydroxy azobenzenes,[55–56] tetra-*ortho*-methoxy azonium ions,[57–58] tricyanofuran-based compounds,[59] and merocyanine photoacids (hereafter referred to as MCHs)—which are nothing but BIPS derivatives in their corresponding open protonated form. In azobenzene-based systems, the difference in acidity is due to dissimilar hydrogen bonding interactions in the corresponding *trans* and *cis* isomers, whereas in MCHs it emerges from the occurrence of an intramolecular cyclization reaction between the (electrophilic) indolium moiety and the (weakly acidic and nucleophilic) phenol moiety accompanied by the release of a proton (Figure 1b). As we will see later in more detail, the apparent acidity difference between the ground state and metastable state of MCHs in water can attain 4 p*K* units,

Cristian Pezzato obtained his PhD in Chemistry in 2015 at the University of Padova (UniPD), Italy, working on nanoparticle-based systems for recognition and catalysis with Prof. Leonard J. Prins. Afterwards, he spent three years (2015-2018) in the laboratory of Nobel Laureate Prof. Sir J. Fraser Stoddart at the Northwestern University, United States, focusing on the design and synthesis of mechanically interlocked molecules, molecular machines and redox systems for battery technology. From 2019 to 2022, he was an "Ambizione" group leader at the Swiss Federal Institute of Technology in Lausanne (EPFL), Switzerland, where he felt in love with the chemistry of merocyanine photoacids. He recently joined the Laboratory for Macromolecular and Organic Chemistry (MOC) at UniPD as Tenure-Track Assistant Professor. His current research encompasses the synthesis and characterization of molecular switches and the development of devices for solar energy harvesting.

Cesare Berton obtained his BSc and MSc degree in Chemistry at the University of Padova, working on the design, synthesis and characterization of supramolecular cages under the supervision of Prof. Cristiano Zonta. In 2019, he started his PhD studies at the Swiss Federal Institute of Technology in Lausanne (EPFL), Switzerland, where he focussed his attention on dissecting the thermodynamics and kinetics of merocyanine photoacids under the guidance of Dr. Cristian Pezzato. He madly loves supramolecular chemistry, NMR spectroscopy and photography.

whereas the photo-induced proton dissociation can last for minutes. If persistent proton dissociation does not occur—as, for example, in polar aprotic solvents such as acetonitrile[60]—molecules with compatible basicity can reversibly uptake the proton to assist the ring-closure.[61–62] In other words, any MCH can be used to perturb acid-base equilibria featuring an equilibrium constant that is higher than that of its ground state, but lower than that of its metastable state.[63] A recent work by Wachtveitl and co-workers,[25] however, suggests that the phenolic site of MCHs can be regarded to as a "super-photoacid"[64] and deprotonation precedes any other thermal decay (see below for a more detailed discussion). Hence, the unrivalled capability of MCHs to display persistent proton dissociation in water results from the possibility to photochemically populate a conjugate base that is metastable. But what are the prerequisites necessary for MCHs to give rise to measurable pH changes? If we assume that i) the ground state equilibrium is quantitatively shifted to the MCH form and ii) visible light absorption leads to quantitative isomerization of MCH into SP and H^+, the resulting pH change can be approximated as [Eq. (1)]:

$$\Delta\mathrm{pH} = \log\sqrt{\frac{C_a}{K_a^{GS}}} \quad (1)$$

where ΔpH corresponds to the pH difference accessible during light irradiation (*i.e.*, pH_{dark}–pH_{light}), whereas C_a indicates the concentration of the MCH form and K_a^{GS} the corresponding ground state acidity constant. It follows that photoinduced proton dissociation in water can be observed only when C_a is higher than K_a^{GS}—*i.e.*, ΔpH can be non-zero and positive only when $C_a \gg K_a^{GS}$. In the case the aqueous equilibrium distribution is not quantitatively shifted towards the MCH form, C_a should be higher than the proton concentration in the dark for observing acidification upon light irradiation. In general, however, water-solubility is poor,[65] and the condition above can be satisfied by making BIPS derivatives that are highly water-soluble[66] and/or whose MCH form is weakly acidic in the dark.[67] This Review will examine the progress done since the discovery of MCHs' reversible proton release, giving particular emphasis to their applications and physicochemical characterization in water.[68]

2. BIPS Photoacidity in Water: Applications

Evidence that MCHs can display reversible proton dissociation in solution emerged as early as 1969 when Shimizu and co-workers[69] reported on the light-triggered proton relay between 6-nitro BIPS and malonic acid in acetone. They showed that the addition of malonic acid to a solution of 6-nitro BIPS produces the corresponding MCH form (as malonate salt) in the dark, and that the system can be driven back to the SP form (and malonic acid) by light irradiation. At the turn of the 21st century, similar results were obtained in water as well by either Braslavsky,[70] who studied the ring closure of MCH in the presence of malonic acid by laser-induced optoacustic spectroscopy, and Willner,[71–73] who showed that MCH moieties anchored onto monolayer surfaces can directly isomerizes to SP following visible light absorption. Direct proofs of the reversible proton dissociation of MCHs in water, however, did not appear before 2004, when Sumaru and co-workers[74] first demonstrated, with pH measurements, that BIPS-functionalized poly(N-isopropylacrylamide) polymers can be used to lower the pH of their aqueous solutions by approximately 1 pH unit. Later on in 2011, these results were consolidated by the seminal work of Liao and co-workers,[67] who showed that a specific non-activated BIPS—bearing a propyl-sulfonate group in position 1′ and lacking the nitro group in position 6—can be used to drive reversible pH changes in water as high as ca. 2 pH units following blue light absorption. Looking more closely at these two seminal examples, it is interesting to note that C_a was almost the same (ca. 0.2 mM), whilst the corresponding pK_a^{GS} values were estimated to be both close to neutrality (ca. 6–7)—*i.e.*, the prerequisite for having pH jumps emerging from Eq. (1) ($C_a \gg K_a^{GS}$) is satisfied. Since Liao's contribution, the use of MCHs to reversibly control acid-base reactions has gained momentum. In the following sections we try to give, to the best of our knowledge, an overview of what has been achieved using MCHs as metastable-state photoacids in water.

2.1. Control of bio-related systems

Water-soluble MCHs are biocompatible compounds[75] and their pH switch can be used as tool for tweaking and controlling the properties of various bio-related proton-sensitive systems. MCHs have been shown to provide a means for biomimetic photoactuation (Figure 2a). For example, Faul and co-workers[76] engineered a device[77] capable of replicating the behaviour of the Cornish mallow—a plant that reorients its leaves according to the position of the light source. Their device features a MCH-containing hydrogel matrix which contracts/expands depending on light-induced pH changes. The geometry of the device was designed such that only the light-exposed part contracts due to the shrinking of the hydrogel matrix. Upon reaching the maximum exposure position, the force exerted by the opposite side of the gel matrix blocks the movement. MCHs can be coupled also with transmembrane ion channels (Figure 2b). The group of Dougherty[78] have used MCHs to control the activation of an ASIC2a acid-sensitive ligand-gated ion channel (GLIC). They employed a sulfonated MCH displaying exceptional water-solubility and that was not interfering with the biochemistry associated to the GLIC. To prove the effective triggering of the channel upon irradiation, the experiments were designed so to force oocytes from *Xenopus laevis* to express the GLICs, and to these cells was applied a solution of photoacid. The electrophysiology traces showed no current in the dark, while under 455 nm irradiation there was a strong and immediate response due to the protonation and the opening of the ion-channels, which could easily be reverted under dark conditions.[78] MCHs have found use also in the reversible actuation of microbial fuel cells (Figure 2c). In the work of Z. Li and co-workers,[79] MCHs

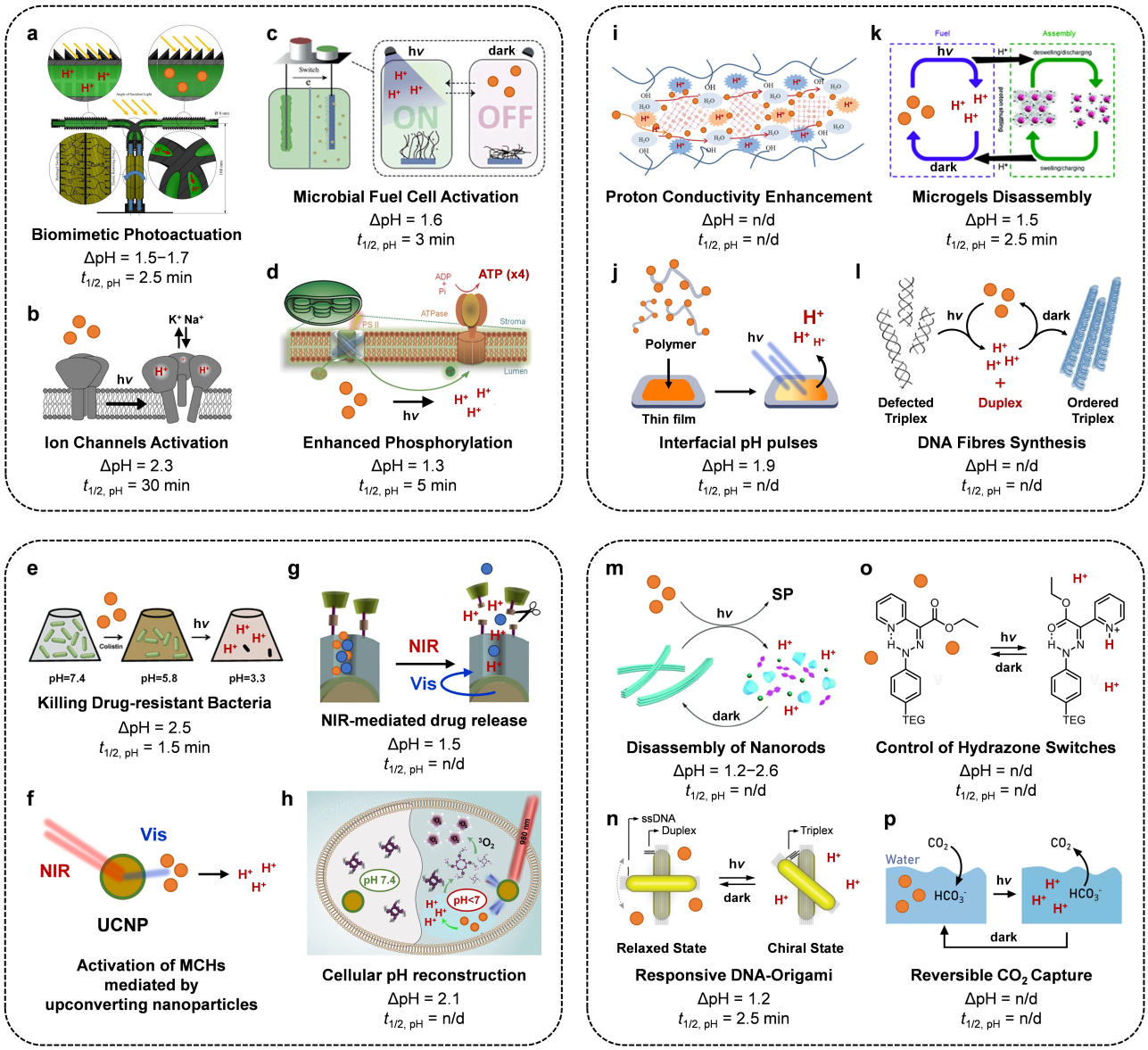

Figure 2. MCHs' capability of triggering reversible pH changes in water has found applications in biochemistry (top left panel, a–d), medicinal chemistry (bottom left panel, e-h), materials science (top right panel, i–l), and systems chemistry (bottom right panel, m-p). The graphics reported here were made from scratch or adapted with permission from (a) Ref. [77], Copyright (2014) IOPscience; (b) Ref. [78], Copyright (2016) Wiley; (c) Ref. [79], Copyright (2014) Royal Society of Chemistry; (d) Ref. [80], Copyright (2017) Wiley; (e) Ref. [81], Copyright (2013) Royal Society of Chemistry; (g) Ref. [84], Copyright (2020) Elsevier; (h) Ref. [85], Copyright (2020) Royal Society of Chemistry; (i) Ref. [86], Copyright (2022) Wiley; (k) Ref. [89], Copyright (2018) Royal Society of Chemistry; (m) Ref. [95], Copyright (2017) Royal Society of Chemistry; (n) Ref. [96], Copyright (2021) Wiley; (p) Ref. [100], Copyright (2017) Elsevier. Below each graphics we have reported the observed pH jump (ΔpH) and its corresponding half-life ($t_{1/2, pH}$) for comparison; in some cases, however, these two parameters were not defined experimentally (n/d).

interferes with the surface chemistry of an ITO electrode bearing a pH-sensitive poly(4-vinyl pyridine)-modified interface, resulting in fast and effective current modulation. This study showcases the opportunity to switch the activity of microbial fuel cells in a fully reversible manner without the need for stepwise addition of acids or bases, which can lead to the accumulation of waste products in the power cell.[79] The group of J. Li[80] has demonstrated that MCHs can be easily actuated inside chloroplasts (Figure 2d). Chloroplasts convert light into a proton-motive force, which in turn is used to produce ATP, thus fixating the energy of light into phosphoanhydride bonds. The extent of this conversion depends on the size of the proton gradient across the thylakoid membrane. Incorporation of MCHs inside chloroplasts resulted in enhanced ATP synthesis following visible light irradiation (4-fold compared to native organelles).[80]

2.2. Opportunities in medicinal chemistry

Visible and NIR light-sensitive systems capable of promoting selective chemical transformations are viable for targeted drug delivery, disinfection and for addressing solubility or aggregation issues. Right after their seminal work in 2011, Liao and co-workers[81] reported on the possibility of exploiting MCHs for inactivating the growth of multidrug-resistant bacteria (Figure 2e). They showed that reversible pH jumps from pH 5.8 to pH 3.3 can be used to kill different strains of *Pseudomonas Aeruginosa*-which are bacteria responsible for many hospital-related infections-by inhibiting the synthesis of intracellular proteins at low pH. It was also shown that combination of MCHs with colistin (a peptide antibiotic) decreased the minimum inhibition concentration of the latter by more than one order of magnitude (ca. 30 times).[81] Utilizing MCHs in vivo is a challenging task because the optical density of living tissues limits[82] the penetration of visible light. Upconversion nanoparticles[83] (UCNPs), however, have been shown to successfully mediate the activation of MCHs. UCNPs are nanoparticles that can absorb multiple low-frequency photons and convert them into one high-frequency photon—for example, two NIR photons into one visible photon (Figure 2f). An interesting example has been reported by Hou and co-workers,[84] who showed that porous cyclodextrin-capped UCNPs and MCHs can be used in the targeted release of doxorubicin-a well-known DNA intercalating agent. Irradiation of UCNPs with NIR photons generated light of suitable wavelength to trigger the photoreaction of MCH, which in turn caused the cleavage of the cyclodextrin capping groups and the subsequent release of doxorubicin molecules (Figure 2g).[84] A similar strategy was adopted by Bu and co-workers,[85] who used a combination of UCNPs and MCHs to reversibly protonate tetraphenylporphirins (TPPs) in biologically relevant conditions by using NIR light (Figure 2h). Typically, TPPs suffer from low solubility at physiological pH and their aggregates have low activity in $^1O_2$ generation. Introduction of alkylamino sidechains on the phenyl rings of TPPs prevented their aggregation at low pH following protonation of the amino groups. It turned out that NIR-generated protons can be used to hinder the aggregation of TPPs thus keeping $^1O_2$ generation at peak performance in biologically relevant conditions. Cytotoxicity assays have shown a 10-fold tumor growth inhibition as compared to the same untreated cell culture.[85]

2.3. Control of materials' properties

Direct incorporation of MCHs into materials has been shown to allow for tuning a variety of acid-base sensitive systems. MCHs can easily be adsorbed within MOFs to regulate their proton sensitivity. Zhang and co-workers,[86] for example, have recently shown that introduction of MCHs in Zinc oxalate-based MOFs enabled the reversible switching of proton conductivity of this composite material (Figure 2i). Under visible light irradiation, the material featured higher conductivity and the process could be reverted simply by stopping the light irradiation.[86] Solid-state photoacid-doped materials have also been reported by Liao and co-workers,[87] who prepared MCH-functionalized methacrylate polymers (Figure 2j). Such polymeric materials were characterized in PBS aqueous buffer solutions utilizing optical spectroscopy and potentiometry. They found that micrometric films of these polymers can induce temporary pH pulses of the supernatant of about 1.9 pH units. The observed proton release revealed to be extremely fast and reversible.[87] The same group has shown the possibility to exploit MCHs in the development of photochromic materials: incorporation of aqueous solutions of MCHs together with bromocresol green in a thin film of polycaprolactone resulted in a very optically dense material which became almost transparent following visible light irradiation.[88] MCHs can also be used to regulate gelation and aggregation processes. The group of Kuehne[89] has prepared a colloidal microgel which could respond to acid-base stimuli, melting into its building blocks at acidic pH values (Figure 2k). This material was described as a dissipative self-assembling system, since the energy delivered by photons is then slowly released as heat during proton reuptake, which led to the re-constitution of the colloidal state.[89] In the group of Sleiman,[90] MCHs were used as proton source for reorganization and error-correction of polyadenine coagulates. Visible light irradiation resulted in protonation of the polyadenines and so in their disassembly. The disassembled structures can subsequently undergo reorganization in a highly ordered aggregation state once the light is switched off (Figure 2l). In other words, the system is pushed away from equilibrium (defected triplex) to form a protonated intermediate (duplex), and once the light source is stopped, the duplex state decays, yielding a more ordered final state (ordered triplex).[90] Very recently, we[91] and others[92] have demonstrated the possibility of using MCHs to mediate and fine tune the assembly of a variety of different DNA nanostructures. In the context of nanomaterials, Ikkala and co-workers[93] prepared hydrogels capable of responding to either temperature and light stimuli in a programmable fashion. Temperature changes or light-induced pH changes can confer different forms to the hydrogel due to different reactive pathways.[93] Similarly, Li and co-workers[94] used MCHs for changing the aggregation state of proton-sensitive materials like chitosan. In this case, the light-induced pH change was exploited for protonating the amino groups on the polysaccharide, which in turn act as ionic groups for scavenging the resulting SP anions. This resulted in the formation of many single-strands of SP-chitosan ion pairs which assemble into supramolecular nanoparticles. The system disassembles spontaneously into its constitutive parts in the dark, thus allowing cyclability.[94]

2.4. Control of chemical and supramolecular systems

The chemistry of MCHs can be exploited for controlling acid-sensitive chemical and supramolecular systems in water. The group of Liu[95] reported on the reversible disassembly of supramolecular nanothreads constituted by subunits of Zn coordinated to 4,4′-bipyridine included in β-cyclodextrins (2 m).

Protonation of the bipyridine basic sites decreases the affinity for the metal ion and the supramolecular structure collapses into its building blocks. Once the irradiation is stopped, the system slowly reverts to the nanothread-shaped state.[95] Kuzyk and co-workers[96] used MCHs to control the shape of DNA-origami (Figure 2n). In this example pairs of gold nanorods were threaded together and functionalized on one end with a pH responsive DNA lock. While resting at pH close to neutrality these assemblies show weak CD signals indicating low concentration of chiral chromophores. Upon irradiation, the system gets locked in a highly asymmetric state as indicated by an intense CD signal.[96] Aprahamian and co-workers[97] reported a hydrazone switch which can be activated by protonation using MCHs (Figure 2o). In their work, the reported hydrazone switch is found in a E/Z ratio of approximatively 6:4 according to NMR studies. Upon MCHs-mediated protonation, the switch gets locked into the Z isomer and slowly decays back to the original equilibrium distribution in the dark.[97] MCHs' photoacidity can contribute also to the development of novel analytical methods. The group of Chumbimuni-Torres,[98] for example, developed MCHs-based systems for ion-sensing. Specifically, they embedded MCHs into a polymeric matrix which is capable of releasing protons under light irradiation creating room for accommodating Ca^{2+} ions. The material showed differences in optical spectra which can be ascribed to the presence of the cation, thus enabling its detection.[99] Remarkably, MCHs may find use also in novel eco-friendly solutions of chemical scavenging and energy harvesting systems. For example, the group of Puxty[100] has shown that, even if to a small extent, carbon dioxide can be desorbed reversibly from aqueous solutions containing MCHs (Figure 2p). The protons released by MCHs lowered the pH value, thus promoting the controlled release of carbon dioxide upon irradiation.[100] Very recently, Kim and co-workers have also shown the possibility of using the proton gradients resulting from MCHs in the development of simple and cost-effective solar energy harvesting system.[101]

3. BIPS photoacidity in water: characterization

As we have seen in the above sections, MCHs can be used to control in principle any acid-sensitive system. Understanding MCHs' mechanisms of action in water, however, is not as easy and intuitive as implementing them as light-responsive cofactors for controlling acid-base equilibria. Until recently, the vast majority of physicochemical studies in water[66,102–104] focussed on simple comparative evaluations at a few selected pH values, rather than exploring systematically the effect of pH for getting mechanistic insights. Gaining a firm grasp of MCHs physicochemical properties is of crucial importance not only from a fundamental point of view, but also for enlarging their applicability further. These considerations have been at the heart of some methodologies we recently developed, thanks to which we have contributed to rationalize several aspects of the thermodynamics and kinetics of MCHs in water.[105] Hereafter, we summarize our efforts in this direction together with other recent findings by other groups.

3.1 Dark acidity

As mentioned above, the aqueous equilibrium distribution of MCHs in the dark is dictated by the pH of their solution. Depending on the substitution pattern of the indoline and the phenol rings, the ground state acidity constant of MCHs can differ by up to 3 p*K* units. For example, electron-withdrawing groups (*e.g.*, NO_2) in position 6 can decrease the pK_a^{GS} to values close to 4,[102] whereas substitution of position 5′ with electron donating groups (*e.g.*, OMe) can increase the pK_a^{GS} to values close to neutrality.[106] If we decide to operate at an intermediate pH of 6, for example, the former MCH will deprotonate quantitatively and will spontaneously isomerize into the corresponding SP form. Besides, the latter will reside almost exclusively in its protonated state and may release proton following light irradiation. Determining the pK_a^{GS} of MCHs accurately is thus of paramount importance for exploring their pH switch potential. To unambiguously quantify the equilibria taking part in solution, we opted for ^{1}H NMR spectroscopy. We acquired NMR spectra at increasing pH values and observed that the equilibrium distribution in the dark progressively shifted from MCH to not only MC, but also SP (Figure 3a).[105] In other words, as the pH increase, dissociation of MCH is followed by isomerization of MC into the corresponding closed SP form. Accurate analysis of both chemical shifts and integrals perturbations (Figure 3b) allows to calculate both the acidity constant of the phenol moiety (K_a) and the isomerization constant of MC into SP (K_c).[105] K_a can be estimated from the observed pH-dependent profile of the chemical shifts associated to the MCH/MC couple ($\delta_{MCH/MC}$), which, at any pH, can be considered as the weighted average of those associated to MCH (δ_{MCH}) and MC (δ_{MC}) [Eq. (2)]:

$$\delta_{MCH/MC} = \frac{[H^+]\delta_{MCH} + K_a\delta_{MC}}{[H^+] + K_a} \quad (2)$$

On the other hand, both K_a and K_c can be determined from the observed integral perturbation in favour of SP [Eq. (3)]:

$$\frac{I_{SP}}{I_{MCH/MC}} = \frac{K_c}{\left(1 + \frac{[H^+]}{K_a}\right)} \quad (3)$$

Since it is evident that the apparent ground state acidity constant of MCHs refers to a three-component equilibrium system, and that the proton concentration at equilibrium must satisfy the charge balance (*i.e.*, $[H^+] = [MC] + [SP]$), it follows that $K_a^{GS} = K_a(1 + K_c)$.[107] Similar pH titrations but performed by UV-Vis spectroscopy (Figure 3c) allows to have a direct guess of pK_a^{GS}, so as to validate the K_a and K_c values determined by NMR.[104] In general, we[105–106] and others[108] have found that the pK_a of MCHs lacking electron withdrawing groups on the phenol ring is similar to that of 4-nitrophenol (7.0–7.4), while their K_c can vary considerably by one order of magnitude (from 2 to 30) depending on the nature of the alkyl bridge and the aromatic substitution of the indoline side, resulting in pK_a^{GS} close to neutrality (6–7).

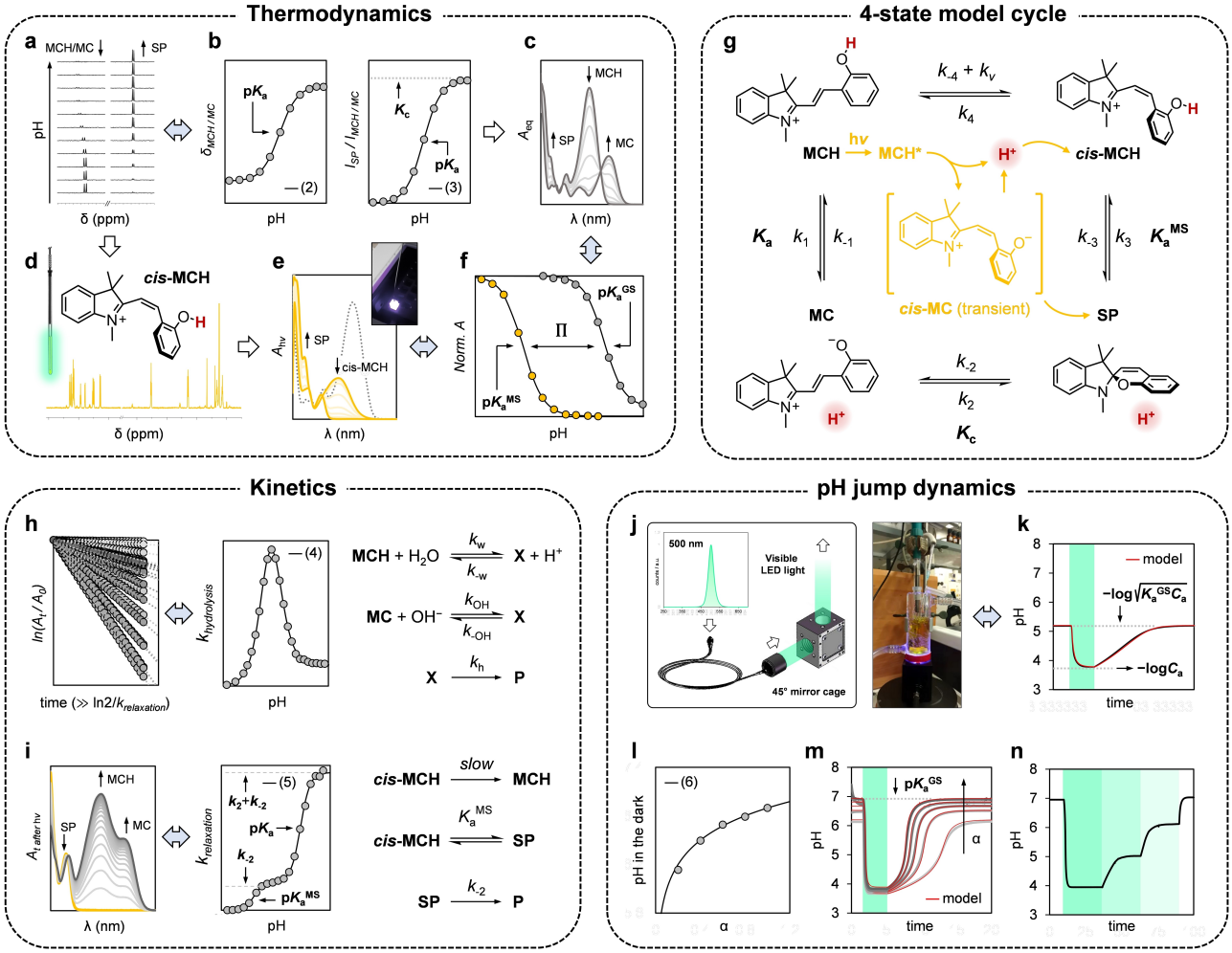

Figure 3. Physicochemical characterization of MCHs in water. (a-f) Workflow for the quantification of the photoacidity. (g) Four-state model describing the operation of MCHs in water with a possible interpretation of the excitation/decay pathways. (h) Kinetics of hydrolysis as a function of the pH and proposed mechanism. (i) Kinetics of relaxation after light irradiation as a function of the pH and proposed mechanism. (j) Photochemical reactor setup for pH jump studies. (k) Representative pH jump dynamics of MCHs. (l) Representative trend of the pH of MCHs solutions recorded under dark equilibrium conditions and as a function of α. (m) Representative pH jump dynamics of MCHs as a function of α. (n) pH tuning by modulation of the light source power. Solid black lines represent the best fit to the corresponding model equation, whereas solid red lines represent the best fit to the four-state cyclic model.

3.2. Photoacidity

To unveil the acid-base pair constituting the metastable state of MCHs in water, we performed ^{1}H NMR spectroscopic analyses under steady light irradiation (*i.e.*, photo NMR studies[109–111]).

We acquired NMR spectra at different pHs and observed that at sufficiently low pH values light irradiation results in the formation of an achiral species featuring a *cis*-non-coplanar conformation, which can be ascribed to *cis*-MCH (Figure 3d).[21,112–113] The coupling constant associated to the corresponding alkenyl hydrogens (13.0 Hz) was found to be in good agreement with those reported earlier by Li[21] (13.5 Hz) and Browne[114] (12.8 Hz) in polar protic solvents. Interestingly, it is also very similar to the one observed by Andréasson[115] (12.8–13.2 Hz) for O-substituted merocyanines after light irradiation. On the other hand, at relatively higher pH values, we confirmed the formation of the chiral spiro form, SP. Similar experiments but performed by UV-Vis spectroscopy at increasing pH values allows to have a direct esteem of the apparent acidity constant of the metastable state (pK_a^{MS}), which is evoked to be the result of a coupling between processes of isomerization and deprotonation occurring photochemically. In fact, the clear isosbestic points observed under steady light irradiation suggests that *cis*-MCH and SP are in photochemical equilibrium (Figure 3e).[105] In general, we found that the pK_a^{MS} of BIPS lacking the common nitro group in position 6 settles at values from 2 to 3 depending on either the substitution pattern of the aromatic rings or the nature of the alkyl bridge. It should be noted, however, that pK_a^{MS} values strongly depend upon both the intensity and the wavelength of the light stimulus to an extent that correlates with the optical overlap with the ground state.[106]

In an analogy with excited-state photoacids,[116] we proposed to define the photoacidity of MCHs (labelled with the Greek symbol Π) as the difference between pK_a^{GS} and pK_a^{MS} (Figure 3f). For all MCHs we examined so far, we found that Π lays around 3.6 pK units and the dynamic of proton release/

uptake is consistent with a four-state dynamic model as the one depicted in Figure 3g (see below for more details). Similar results have been obtained by Andréasson[102] ($\Pi = 3.5 \pm 0.6$) and Beves[108] ($\Pi = 3.5 \pm 0.3$) on a series of differently substituted compounds including 6-nitro BIPS derivatives.

A key open question regarding the operation of MCHs in water, however, is whether deprotonation occurs before, during or as a consequence of photoisomerization. After a series of pioneering studies,[117–119] Wachtveitl, Heckel and co-workers[25] have recently performed transient absorption spectroscopy (TAS) studies on a series of activated BIPS derivatives, showing that the phenol moiety can behave as a super photoacid. Their experiments were carried out at pH 1 to quantitatively shift the equilibrium distribution towards the corresponding open protonated form in the dark ($pK_a^{GS} = 3.7$). They found that the excited state of MCH (MCH*) deprotonates within a few picoseconds and the resulting MC* rapidly decays to its ground state MC (10-100 ps) before proton recombination; the pK_a of the excited state was estimated by the Foster cycle model to be around −4.2, reflecting a pK_a drop of almost 8 p*K* units.[25] Given the relatively high acidity of the examines compounds, though, the pH range of these experiments might haven't been low enough for probing cisoid protonated species (see above). In any case, these results strongly suggest that deprotonation occurs before photoisomerization. Very recently, Sension and co-workers[24] have performed TAS experiments using their propyl-sulfonated derivative at intermediate pH values (pH 5.5) and observed that deprotonation is followed by the formation of a relatively long-lived *cis*-deprotonated form (*cis*-MC) prior to SP formation.[24] Similar results have been reported by Beves and co-workers, who showed that the *cis*-MC intermediate species displays a lifetime between 30 and 550 nanoseconds depending on the molecular structure.[108] These results, in conjunction with the photo NMR studies described above, suggest that visible light absorption trigger the formation of *cis*-MC after deprotonation, so as to produce SP or *cis*-MCH following ring closure or proton recombination when the pH is sufficiently low, respectively (see the yellow scheme in the middle of Figure 3g). We anticipate that further mechanistic insights might be obtained by systematically performing TAS or isomerization kinetic experiments as a function of the pH.

3.3. Hydrolysis

The major drawback when using MCHs in water is the fact they tend to hydrolyse irreversibly. The effect of pH on the hydrolysis kinetics, however, has always been something quite overlooked in favour of simpler studies under extremely acidic or basic conditions (*e.g.*, at pH 3 or 10).[66] As a result, the mechanism of hydrolysis has been subjected to different interpretations. From our side, we performed kinetic experiments at varying pH on a series of different MCHs and found that, in all cases, the apparent first-order rate constant of hydrolysis ($k_{hydrolysis}$) gradually increases until a maximum close to pH values approaching their pK_a^{GS}, where it starts to decrease to become progressively independent of pH (Figure 3h).[105] Such bell-shaped profiles are reminiscent of those commonly observed for the hydrolysis of Schiff bases and, similarly, we ascribed them to a change in the rate determining step from decomposition of a tetrahedral intermediate (k_h) to nucleophilic addition of water (k_w, or hydroxide ions, k_{OH}) at higher pH values. The expression for the rate of hydrolysis, which can be easily derived by applying the steady state approximation [Eq. (4)]:

$$k_{hydrolysis} = \frac{k_w[H^+] + k_{OH}K_w}{([H^+] + K_a^{GS})\left(\frac{k_{-w}}{k_h}[H^+] + 1\right)} \quad (4)$$

fits well the experimental profiles. Interestingly, we found that substitution of either the indoline or the phenol ring with electron donating groups (*e.g.*, OMe[104]) directly conjugated to the ene-iminium core disfavours nucleophilic attacks and increases the stability of MCHs by up to 4 times.[106] Previous findings[65,120–121] have also suggested that the chemical stability of the MCH form can be significantly enhanced through supramolecular interactions, but as of now there are no studies about the effect of encapsulation on the proton photo-release. We anticipate that selective encapsulation of the MCH form may increase its chemical stability without affecting the capability of reversibly releasing protons following light irradiation.

3.4. Metastability

The most appealing feature of MCHs, which is at the heart of their wide-spreading applicability as photoacids, is the lifetime of their proton-photodissociated state. Beginning from the first contributions by Liao on this matter, it was shown that the relaxation towards equilibrium in water followed first order kinetics at intermediate pH values.[67] This first observation soon left the scene after some studies in polar organic solvents, which suggested protonation is involved in the rate determining step of relaxation. The fact the extrapolated second order rate constants[103,122] were increasing proportionally with the hydrogen bond donor acidity of the solvent[123] made such a hypothesis generally accepted. To check whether proton is effectively involved in the rate determining step of the reaction in water, we examined the relaxation kinetics of MCHs after irradiation over the entire pH window.[105] In all cases, we found that the apparent rate constant of relaxation in the dark ($k_{relaxation}$) progressively increases with pH following bi-sigmoidal profiles displaying two inflection points at pH values close to the corresponding pK_a^{MS} and pK_a (Figure 3i). The four-state kinetic cycle (Figure 3g), where $k_1/k_{-1} = K_a$, $k_2/k_{-2} = K_c$, $k_3/k_{-3} = K_a^{MS}$, and k_4 and k_{-4} are the kinetic constants of the *trans*-to-*cis* isomerization of MCH and its reverse reaction in the absence of light (*i.e.*, $k_v = 0$), revealed to be fully consistent with the observed experimental profiles, showing that the photochemically-populated state(s) relax back to equilibrium following preferentially the bottom left corner.[105] One may argue that the half-headed double arrows between MCH and *cis*-MCH is not the right choice on account of the involvement of light (k_v)

in the transformation.[113–114] A recent study by Beves and co-workers, however, has shown that dark equilibrium distributions comprising MCH and *cis*-MCH can be probed by ^{1}H NMR when the pH is sufficiently low.[124] This means that, in accordance with the proposed four-state model and at $pH \ll pK_a^{MS}$, the system can (slowly) relax towards equilibrium also following the top right corner. Some reports on the acidochromism of BIPS have ascribed the low rates observed at acidic pH values to the formation of an "unreactive sink", which was proposed to be the closed spiro form protonated at the indoline's nitrogen atom (*i.e.*, SPH).[17] More recent computational studies, however, excludes such a hypothesis, showing that proton transfer coupled with C–O cleavage is barrierless and result in the formation of *cis*-MCH.[114] Thus, given the apparent stability of the *cis*-MCH form, we reasoned to apply the pre-equilibrium approximation so as to derive a simplified version of the expression for the rate of relaxation [Eq. (5)]:

$$k_{relaxation} = k_{-2}\left(\frac{K_a^{MS}}{[H^+] + K_a^{MS}}\right)\left(\frac{K_a(1 + K_c) + [H^+]}{[H^+] + K_a}\right) \quad (5)$$

Also in this case, we observed a good match between experiments and theory.[105] In other words, our experiments suggest that the proton is not involved in the rate determining step of relaxation: thermal ring opening of SP (k_{-2}) remains rate determining throughout almost the entire pH window, with *cis*-to-*trans* isomerization of *cis*-MCH competing significantly only at extremely low pH values. Our interpretation, though, explains also why the relaxation of MCHs, in pH windows above their corresponding pK_a^{MS}, could fit well a first order rate equation also in the absence of buffers—*i.e.*, in the absence of pseudo first order conditions.[105]

As a side note, if the timescale of hydrolysis and relaxation are similar, a specific bi-exponential rate equation can be used to not only extrapolate both $k_{hydrolysis}$ and $k_{relaxation}$, but also to indirectly quantify both pK_a^{GS} and pK_a^{MS} from pH-dependent relaxation experiments.[125]

3.5. pH jump characterization studies

Multiple aspects need to be considered for correlating the thermodynamic and kinetic parameters discussed above with the pH measurement during dark/light cycles. In this regard, we specifically designed a photochemical reactor comprising a jacketed beaker mounted on top of a 45° mirror cage, which allows for irradiating the solution from the bottom while simultaneously inserting both the pH electrode and a nitrogen inlet from the top (Figure 3j).[105] With this setup, the sample solution can be kept under an inert atmosphere and at a constant temperature, which both are parameters that can affect pH measurements. In fact, contrary to NMR and UV-Vis titrations, which are typically carried out using buffer solutions, here carbon dioxide can significantly alter the pH of the solutions. On the other hand, the use of a jacketed beaker is important not only to prevent temperature rise during light irradiation but also to allow correlation of the pH readings with the apparent acidity constants. Also, operating under stirring and in presence of ionic strength (*e.g.*, KCl 20 mM) is beneficial for maintaining a fast response of the glass electrode throughout the experiments. By taking care of all these aspects, it can be shown that MCHs' aqueous solutions feature pH values close to those expected considering the weak acid approximation (*i.e.*, $pH = -\log(K_a^{GS}C_a)^{1/2}$). On the other hand, depending on the specific solubility of the compound tested, the pH achievable under light irradiation approaches values compatible with quantitative proton dissociation (*i.e.*, $pH = -\log C_a$) (Figure 3k). If the solubility is high enough, however, the pH can further decrease to values close to the corresponding pK_a^{MS}.[105] The entire dynamics of proton release/uptake can be subjected to the four-state model described above to extrapolate the rate constant of the light-triggered perturbation (k_v), from which the quantum yield can be calculated. Generally, we found that MCHs display pH jumps of ca. 1.5 pH units, with a quantum yield spanning from 0.2 to 0.7 depending on the molecular structure.[105] The quantum yield of proton release, however, appeared not be a limiting factor for bulk pH switches.[108] Instead, an important parameter for tuning the amplitude of the pH jumps is the neutralization degree of MCHs (α). In fact, under dark conditions, we have shown that the pH of MCHs' aqueous solutions as a function of α varies according to the Henderson-Hasselbalch equation (Figure 3l) [Eq. (6)]:

$$pH = pK_a^{GS} + \log\frac{\alpha}{(1 - \alpha)} \quad (6)$$

and the corresponding pH jump following 500 nm light absorption can be increased to 3 pH units when starting from $pH = pK_a^{GS}$ (Figure 3m).[106] Similar results have been recently obtained by Beves and co-workers, who reported reversible switches from pH 8.3 to pH 5.2.[124] Altogether, these results show that MCHs can effectively act as "light-switchable buffers", giving rise to pH jumps that can be as high as their photoacidity with exceptional fatigue resistance.[106]

Of note, MCHs constitute one of the few systems[126] for which non-equilibrium states can be probed with direct measurements, as their variable-power pH jumps can be easily measured with a glass electrode (Figure 3n). Perhaps, this is only one of the reasons why further research is yet to come.

4. Conclusions and Outlook

The use of MCHs as reversible photoacids has experienced steady growth over the past decade as it has proved to be instrumental in making a variety of different pH-sensitive systems controllable with light stimuli. Understanding precisely the operation of MCHs in water, however, was far less straightforward. The big picture emerging from recent studies shows that both the ground state and the metastable state are the result of a coupling between processes of deprotonation and isomerization, leading to equilibrium or photostationary distributions characterized by apparent acidity constants that differ by up to 4 p*K* units. The four states of MCHs that are

identified as thermodynamically stable (MCH, MC, *cis*-MCH, and SP) can be linked together in a cyclic model where the proton is released clockwise and taken up anti-clockwise (Figure 3g). This model suits very well the full proton release/uptake dynamics observed experimentally and can be used to make theoretical predictions.

In the future, we believe several aspects need to be considered for this class of reversible photoacids to eventually reach real-world applications. One for all deals with developing long-lasting systems. In this regard, apart from substituent effects[122] it may be beneficial to focus on the establishment of selective non-covalent interactions through either supramolecular encapsulation and confined spaces.[127–130] Second, although we have shown the pH jumps of MCHs can be amplified by partial neutralization, it is not yet clear what the energy transduction efficiency[126] of the proton release is. We predict that systematic pH jump studies as a function of i) concentration, ii) degree of neutralization, and iii) irradiation power will be beneficial in this regard. Last but not least, in line with Eq. (1) above, one may prefer to dramatically increase the solubility in water instead of pK_a^{GS} to explore extremely acidic pH windows. We foresee that this choice may allow for augmenting the current flow in solar energy harvesting devices based on light-triggered proton gradients.[101]

Acknowledgements

This work was supported by the Swiss National Science Foundation (SNSF "Ambizione" PZ00P2_180008). C. P. is thankful for support from the Italian Ministry of Education and Research (Rita Levi Montalcini Program PGR19CX3UP). Open Access funding provided by École Polytechnique Fédérale de Lausanne.

Conflict of Interest

The authors declare no conflict of interest.

Keywords: photochemistry · light-switchable buffers · merocyanine photoacids · photoacidity · reversible pH jumps

[1] V. I. Minkin, in *Molecular Switches*, Vol. 1 (Eds: B. L. Feringa, W. R. Browne), Wiley-VCH, Weinheim, Germany **2011**, pp. 37–80.
[2] L. Kortekaas, W. R. Browne, in *Molecular Photoswitches*, Vol 1 (Ed.: Z. L. Pianowski), Wiley-VCH, Weinheim, Germany **2022**, pp. 131–149.
[3] L. Kortekaas, W. R. Browne, *Chem. Soc. Rev.* **2019**, *48*, 3406–3424.
[4] H. Bouas-Laurent, H. Durr, *Pure Appl. Chem.* **2001**, *73*, 639–665.
[5] R. Wizinger, H. Wenning, *Helv. Chim. Acta* **1940**, *23*, 247–271.
[6] Y. Hirshberg, E. Fischer, *J. Chem. Soc.* **1954**, 297–303.
[7] Y. Hirshberg, E. Fischer, *J. Chem. Soc.* **1954**, 3129–3137.
[8] R. Heiligman-Rim, Y. Hirshberg, E. Fischer, *J. Chem. Soc.* **1961**, 156–163.
[9] R. Heiligman-Rim, Y. Hirshberg, E. Fischer, *J. Phys. Chem.* **1962**, *66*, 2465–2470.
[10] R. Heiligman-Rim, Y. Hirshberg, E. Fischer, *J. Phys. Chem.* **1962**, *66*, 2470–2477.
[11] P. H. Vandewyer, J. Hoefnagels, G. Smets, *Tetrahedron* **1969**, *25*, 3251–3266.
[12] N. W. Tyer, Jr., R. S. Becker, *J. Am. Chem. Soc.* **1970**, *92*, 1289–1294.
[13] A. Samat, D. De Keukeleire, R. Guglielmetti, *Bull. Soc. Chim. Belg.* **1991**, *100*, 679–700.
[14] V. I. Minkin, *Chem. Rev.* **2004**, *104*, 2751–2776.
[15] J. H. Day, *Chem. Rev.* **1963**, *63*, 65–80.
[16] W. G. Tian, J. T. Tian, *Dyes Pigm.* **2014**, *105*, 66–74.
[17] J. T. C. Wojtyk, A. Wasey, N. N. Xiao, P. M. Kazmaier, S. Hoz, C. Yu, R. P. Lemieux, E. Buncel, *J. Phys. Chem. A* **2007**, *111*, 2511–2516.
[18] A. V. Chernyshev, N. A. Voloshin, I. A. Rostovtseva, O. P. Demidov, K. E. Shepelenko, E. V. Solov′eva, E. B. Gaeva, A. V. Metelitsa, *Dyes Pigm.* **2020**, *178*.
[19] J. D. Steen, D. R. Duijnstee, A. S. Sardjan, J. Martinelli, L. Kortekaas, D. Jacquemin, W. R. Browne, *J. Phys. Chem. A* **2021**, *125*, 3355–3361.
[20] T. A. Kim, M. J. Robb, J. S. Moore, S. R. White, N. R. Sottos, *Macromolecules* **2018**, *51*, 9177–9183.
[21] J. W. Zhou, Y. T. Li, Y. W. Tang, F. Q. Zhao, X. Q. Song, E. C. Li, *J. Photochem. Photobiol. A* **1995**, *90*, 117–123.
[22] J. Buback, M. Kullmann, F. Langhojer, P. Nuernberger, R. Schmidt, F. Wurthner, T. Brixner, *J. Am. Chem. Soc.* **2010**, *132*, 16510–16519.
[23] S. Ruetzel, M. Diekmann, P. Nuernberger, C. Walter, B. Engels, T. Brixner, *J. Chem. Phys.* **2014**, *140*, 224310.
[24] C. R. Aldaz, T. E. Wiley, N. A. Miller, N. Abeyrathna, Y. Liao, P. M. Zimmerman, R. J. Sension, *J. Phys. Chem. B* **2021**, *125*, 4120–4131.
[25] C. Kaiser, T. Halbritter, A. Heckel, J. Wachtveitl, *Chem. Eur. J.* **2021**, *27*, 9160–9173.
[26] A. K. Chibisov, H. Gorner, *Phys. Chem. Chem. Phys.* **2001**, *3*, 424–431.
[27] H. Gorner, *Phys. Chem. Chem. Phys.* **2001**, *3*, 416–423.
[28] S. R. Keum, K. B. Lee, P. M. Kazmaier, E. Buncel, *Tetrahedron Lett.* **1994**, *35*, 1015–1018.
[29] P. Joseph, K. Kundu, P. K. Kundu, *ChemistrySelect* **2018**, *3*, 11065–11070.
[30] V. A. Barachevsky, *Rev. J. Chem.* **2017**, *7*, 334–371.
[31] R. Klajn, *Chem. Soc. Rev.* **2014**, *43*, 148–184.
[32] F. M. Raymo, S. Giordani, *J. Am. Chem. Soc.* **2001**, *123*, 4651–4652.
[33] F. M. Raymo, S. Giordani, A. J. White, D. J. Williams, *J. Org. Chem.* **2003**, *68*, 4158–4169.
[34] X. Xie, E. Bakker, *J. Am. Chem. Soc.* **2014**, *136*, 7857–7860.
[35] X. Xie, G. A. Crespo, G. Mistlberger, E. Bakker, *Nat. Chem.* **2014**, *6*, 202–207.
[36] P. T. Chou, K. M. Solntsev, *J. Phys. Chem. B* **2015**, *119*, 2089–2089.
[37] A. Fagan, M. Bartkowski, S. Giordani, *Front. Chem.* **2021**, *9*, 720087.
[38] A. Towns, *Phys. Sci. Rev.* **2021**, *6*, 341–368.
[39] J. K. Rad, Z. Balzade, A. R. Mahdavian, *J. Photochem. Photobiol. C* **2022**, *51*.
[40] G. Berkovic, V. Krongauz, V. Weiss, *Chem. Rev.* **2000**, *100*, 1741–1754.
[41] A. S. Kozlenko, I. V. Ozhogin, A. D. Pugachev, M. B. Lukyanova, I. M. El-Sewify, B. S. Lukyanov, *Top. Curr. Chem.* **2023**, *381*, 8.
[42] D. Mariottini, D. Del Giudice, G. Ercolani, S. Di Stefano, F. Ricci, *Chem. Sci.* **2021**, *12*, 11735–11739.
[43] D. Del Giudice, F. Frateloreto, C. Sappino, S. Di Stefano, *Eur. J. Org. Chem.* **2022**, *2022*, e202200407.
[44] V. Balzani, G. Bergamini, P. Ceroni, *Angew. Chem. Int. Ed.* **2015**, *54*, 11320–11337; *Angew. Chem.* **2015**, *127*, 11474–11492.
[45] M. Shirai, M. Tsunooka, *Prog. Polym. Sci.* **1996**, *21*, 1–45.
[46] J. F. Ireland, P. A. H. Wyatt, in *Adv. Phys. Org. Chem., Vol. 12* (Ed.: V. Gold), Academic Press **1976**, pp. 131–221.
[47] Y. Liao, *Acc. Chem. Res.* **2017**, *50*, 1956–1964.
[48] C. J. Martin, G. Rapenne, T. Nakashima, T. Kawai, *J. Photochem. Photobiol. C* **2018**, *34*, 41–51.
[49] N. A. Kuznetsova, G. V. Malkov, B. G. Gribov, *Russ. Chem. Rev.* **2020**, *89*, 173–190.
[50] O. Gajst, O. Green, L. Pinto da Silva, J. C. G. Esteves da Silva, D. Shabat, D. Huppert, *J. Phys. Chem. A* **2018**, *122*, 8126–8135.
[51] K. Fujii, M. Aramaki, Y. Kimura, *J. Phys. Chem. B* **2018**, *122*, 12363–12374.
[52] R. Nandi, N. Amdursky, *Acc. Chem. Res.* **2022**, *55*, 2728–2739.
[53] R. M. D. Nunes, M. Pineiro, L. G. Arnaut, *J. Am. Chem. Soc.* **2009**, *131*, 9456–9462.
[54] Y. Liao, *Phys. Chem. Chem. Phys.* **2022**, *24*, 4116–4124.
[55] M. Emond, T. Le Saux, S. Maurin, J. B. Baudin, R. Plasson, L. Jullien, *Chem. Eur. J.* **2010**, *16*, 8822–8831.
[56] M. Emond, J. Sun, J. Gregoire, S. Maurin, C. Tribet, L. Jullien, *Phys. Chem. Chem. Phys.* **2011**, *13*, 6493–6499.
[57] S. Samanta, A. Babalhavaeji, M. X. Dong, G. A. Woolley, *Angew. Chem. Int. Ed.* **2013**, *52*, 14127–14130; *Angew. Chem.* **2013**, *125*, 14377–14380.

[58] M. Dong, A. Babalhavaeji, M. J. Hansen, L. Kalman, G. A. Woolley, *Chem. Commun.* **2015**, *51*, 12981–12984.
[59] V. K. Johns, P. Peng, J. DeJesus, Z. Wang, Y. Liao, *Chem. Eur. J.* **2014**, *20*, 689–692.
[60] R. J. Li, C. Pezzato, C. Berton, K. Severin, *Chem. Sci.* **2021**, *12*, 4981–4984.
[61] S. Silvi, E. C. Constable, C. E. Housecroft, J. E. Beves, E. L. Dunphy, M. Tomasulo, F. M. Raymo, A. Credi, *Chem. Commun.* **2009**, 1484–1486.
[62] S. M. Jansze, G. Cecot, K. Severin, *Chem. Sci.* **2018**, *9*, 4253–4257.
[63] J. Vallet, J. C. Micheau, C. Coudret, *Dyes Pigm.* **2016**, *125*, 179–184.
[64] J. Knorr, N. Sulzner, B. Geissler, C. Spies, A. Grandjean, R. J. Kutta, G. Jung, P. Nuernberger, *Photochem. Photobiol. Sci.* **2022**, *21*, 2179–2192.
[65] Z. Miskolczy, L. Biczok, *J. Phys. Chem. B* **2011**, *115*, 12577–12583.
[66] D. Moldenhauer, F. Grohn, *Chem. Eur. J.* **2017**, *23*, 3966–3978.
[67] Z. Shi, P. Peng, D. Strohecker, Y. Liao, *J. Am. Chem. Soc.* **2011**, *133*, 14699–14703.
[68] C. Berton, **2023**. *Dissecting the photoacidity of spiropyran/merocyanine molecular switches in water* (Doctoral dissertation, EPFL, Switzerland); doi: 10.5075/epfl-thesis-10156.
[69] I. Shimizu, H. Kokado, E. Inoue, *Bull. Chem. Soc. Jpn.* **1969**, *42*, 1726–1729.
[70] R. M. Williams, G. Klihm, S. E. Braslavsky, *Helv. Chim. Acta* **2001**, *84*, 2557–2576.
[71] M. Liondagan, E. Katz, I. Willner, *J. Am. Chem. Soc.* **1994**, *116*, 7913–7914.
[72] I. Willner, M. Liondagan, S. Marxtibbon, E. Katz, *J. Am. Chem. Soc.* **1995**, *117*, 6581–6592.
[73] A. Doron, E. Katz, G. L. Tao, I. Willner, *Langmuir* **1997**, *13*, 1783–1790.
[74] K. Sumaru, M. Kameda, T. Kanamori, T. Shinbo, *Macromolecules* **2004**, *37*, 4949–4955.
[75] F. Cardano, E. Del Canto, S. Giordani, *Dalton Trans.* **2019**, *48*, 15537–15544.
[76] M. P. M. Dicker, P. M. Weaver, J. M. Rossiter, I. P. Bond, C. F. J. Faul, in *Bionspiration, Biomimetics, and Bioreplication VI* **2016** (Proceedings of SPIE, Vol. 9797).
[77] M. P. M. Dicker, J. M. Rossiter, I. P. Bond, P. M. Weaver, *Bioinspiration Biomimetics* **2014**, *9*, 036015.
[78] O. S. Shafaat, J. R. Winkler, H. B. Gray, D. A. Dougherty, *ChemBioChem* **2016**, *17*, 1323–1327.
[79] H. Bao, F. F. Li, L. C. Lei, B. Yang, Z. J. Li, *RSC Adv.* **2014**, *4*, 27277–27280.
[80] Y. Xu, J. Fei, G. Li, T. Yuan, Y. Li, C. Wang, X. Li, J. Li, *Angew. Chem. Int. Ed.* **2017**, *56*, 12903–12907; *Angew. Chem.* **2017**, *129*, 13083–13087.
[81] Y. Luo, C. Wang, P. Peng, M. Hossain, T. Jiang, W. Fu, Y. Liao, M. Su, *J. Mater. Chem. B* **2013**, *1*, 997–1001.
[82] W. A. Velema, W. Szymanski, B. L. Feringa, *J. Am. Chem. Soc.* **2014**, *136*, 2178–2191.
[83] G. Chen, H. Qiu, P. N. Prasad, X. Chen, *Chem. Rev.* **2014**, *114*, 5161–5214.
[84] R. L. Han, S. Wu, K. Q. Tang, Y. F. Hou, *Adv. Powder Technol.* **2020**, *31*, 3860–3866.
[85] C. C. Wang, P. R. Zhao, G. L. Yang, X. Y. Chen, Y. Q. Jiang, X. W. Jiang, Y. L. Wu, Y. Y. Liu, W. A. Zhang, W. B. Bu, *Mater. Horiz.* **2020**, *7*, 1180–1185.
[86] S. F. Zhou, G. M. Wu, C. X. Zhang, Q. L. Wang, *Adv. Mater. Interfaces* **2022**, *9*, 2102147.
[87] A. Elgattar, N. Abeyrathna, Y. Liao, *J. Phys. Chem. B* **2019**, *123*, 648–654.
[88] H. B. Chen, Y. Liao, *J. Photochem. Photobiol. A* **2015**, *300*, 22–26.
[89] D. Go, D. Rommel, Y. Liao, T. Haraszti, J. Sprakel, A. J. C. Kuehne, *Soft Matter* **2018**, *14*, 910–915.
[90] F. J. Rizzuto, C. M. Platnich, X. Luo, Y. Shen, M. D. Dore, C. Lachance-Brais, A. Guarne, G. Cosa, H. F. Sleiman, *Nat. Chem.* **2021**, *13*, 843–849.
[91] V. J. Perillat, E. Del Grosso, C. Berton, F. Ricci, C. Pezzato, *Chem. Commun.* **2023**, *59*, 2146–2149.
[92] L. Wimberger, F. J. Rizzuto, J. E. Beves, *J. Am. Chem. Soc.* **2023**, *145*, 2088–2092.
[93] H. Zhang, H. Zeng, A. Priimagi, O. Ikkala, *Nat. Commun.* **2019**, *10*, 3267.
[94] X. M. Chen, X. F. Hou, H. K. Bisoyi, W. J. Feng, Q. Cao, S. Huang, H. Yang, D. Chen, Q. Li, *Nat. Commun.* **2021**, *12*, 4993.
[95] J. Guo, H. Y. Zhang, Y. Zhou, Y. Liu, *Chem. Commun.* **2017**, *53*, 6089–6092.
[96] J. Ryssy, A. K. Natarajan, J. H. Wang, A. J. Lehtonen, M. K. Nguyen, R. Klajn, A. Kuzyk, *Angew. Chem. Int. Ed.* **2021**, *60*, 5859–5863; *Angew. Chem.* **2021**, *133*, 5923–5927.
[97] L. A. Tatum, J. T. Foy, I. Aprahamian, *J. Am. Chem. Soc.* **2014**, *136*, 17438–17441.
[98] P. K. Patel, V. K. Johns, D. M. Mills, J. E. Boone, P. Calvo-Marzal, K. Y. Chumbimuni-Torres, *Electroanalysis* **2015**, *27*, 677–683.
[99] P. K. Patel, K. Y. Chumbimuni-Torres, *Analyst* **2016**, *141*, 85–89.
[100] R. Bennett, S. Clifford, K. Anderson, G. Puxty, *Energy Procedia* **2017**, *114*, 1–6.
[101] J. Bae, H. Lim, J. Ahn, Y. H. Kim, M. S. Kim, I. D. Kim, *Adv. Mater.* **2022**, *34*, e2201734.
[102] M. Hammarson, J. R. Nilsson, S. Li, T. Beke-Somfai, J. Andreasson, *J. Phys. Chem. B* **2013**, *117*, 13561–13571.
[103] V. K. Johns, Z. Z. Wang, X. X. Li, Y. Liao, *J. Phys. Chem. A* **2013**, *117*, 13101–13104.
[104] N. Abeyrathna, Y. Liao, *J. Phys. Org. Chem.* **2017**, *30*.
[105] C. Berton, D. M. Busiello, S. Zamuner, E. Solari, R. Scopelliti, F. Fadaei-Tirani, K. Severin, C. Pezzato, *Chem. Sci.* **2020**, *11*, 8457–8468.
[106] C. Berton, D. M. Busiello, S. Zamuner, R. Scopelliti, F. Fadaei-Tirani, K. Severin, C. Pezzato, *Angew. Chem. Int. Ed.* **2021**, *60*, 21737–21740; *Angew. Chem.* **2021**, *133*, 21905–21908.
[107] A. V. Chernyshev, M. S. Chernov'yants, E. N. Voloshina, N. A. Voloshin, *Russ. J. Gen. Chem.* **2002**, *72*, 1468–1472.
[108] L. Wimberger, S. K. K. Prasad, M. D. Peeks, J. Andreasson, T. W. Schmidt, J. E. Beves, *J. Am. Chem. Soc.* **2021**, *143*, 20758–20768.
[109] Y. N. Ji, D. A. DiRocco, J. Kind, C. M. Thiele, R. M. Gschwind, M. Reibarkh, *ChemPhotoChem* **2019**, *3*, 984–992.
[110] P. Nitschke, N. Lokesh, R. M. Gschwind, *Prog. Nucl. Magn. Reson. Spectrosc.* **2019**, *114*, 86–134.
[111] J. E. Bramham, A. P. Golovanov, *Commun. Chem.* **2022**, *5*, 90.
[112] C. J. Roxburgh, P. G. Sammes, *Dyes Pigm.* **1995**, *27*, 63–69.
[113] H. Shiozaki, *Dyes Pigm.* **1997**, *33*, 229–237.
[114] L. Kortekaas, J. Chen, D. Jacquemin, W. R. Browne, *J. Phys. Chem. B* **2018**, *122*, 6423–6430.
[115] C. L. Fleming, S. M. Li, M. Grotli, J. Andreasson, *J. Am. Chem. Soc.* **2018**, *140*, 14069–14072.
[116] H. Kagel, M. Frohme, J. Glökler, *J. Cell. Biotechnol.* **2018**, *4*, 23–30.
[117] J. Kohl-Landgraf, M. Braun, C. Ozcoban, D. P. Goncalves, A. Heckel, J. Wachtveitl, *J. Am. Chem. Soc.* **2012**, *134*, 14070–14077.
[118] T. Halbritter, C. Kaiser, J. Wachtveitl, A. Heckel, *J. Org. Chem.* **2017**, *82*, 8040–8047.
[119] C. Kaiser, T. Halbritter, A. Heckel, J. Wachtveitl, *ChemistrySelect* **2017**, *2*, 4111–4123.
[120] Z. Miskolczy, L. Biczok, *Photochem. Photobiol.* **2012**, *88*, 1461–1466.
[121] J. R. Nilsson, C. P. Carvalho, S. M. Li, J. P. Da Silva, J. Andreasson, U. Pischel, *ChemPhysChem* **2012**, *13*, 3691–3699.
[122] J. Liu, W. Tang, L. Sheng, Z. Du, T. Zhang, X. Su, S. X. Zhang, *Chem. Asian J.* **2019**, *14*, 438–445.
[123] D. C. Leggett, *J. Solution Chem.* **1994**, *23*, 697–701.
[124] L. Wimberger, J. Andreasson, J. E. Beves, *Chem. Commun.* **2022**, *58*, 5610–5613.
[125] V. J. Périllat, C. Berton, C. Pezzato, *Mater. Today Chem.* **2022**, *25*, 100918.
[126] S. Corra, M. T. Bakic, J. Groppi, M. Baroncini, S. Silvi, E. Penocchio, M. Esposito, A. Credi, *Nat. Nanotechnol.* **2022**, *17*, 746–751.
[127] M. J. Feeney, S. W. Thomas, *Macromolecules* **2018**, *51*, 8027–8037.
[128] A. B. Grommet, L. M. Lee, R. Klajn, *Acc. Chem. Res.* **2020**, *53*, 2600–2610.
[129] C. Li, A. Iscen, L. C. Palmer, G. C. Schatz, S. I. Stupp, *J. Am. Chem. Soc.* **2020**, *142*, 8447–8453.
[130] J. Wang, L. Avram, Y. Diskin-Posner, M. J. Bialek, W. Stawski, M. Feller, R. Klajn, *J. Am. Chem. Soc.* **2022**, *144*, 21244–21254.

Manuscript received: January 25, 2023
Revised manuscript received: February 27, 2023
Accepted manuscript online: February 27, 2023

REVIEW

Indolinospirobenzopyrans in their open protonated form constitute the archetype of "metastable-state photoacids", as they can release protons persistently and reversibly following visible light absorption. In this Review, we survey their wide-spread applicability by contextualizing the prerequisites underlying the photo-triggered proton release in water.

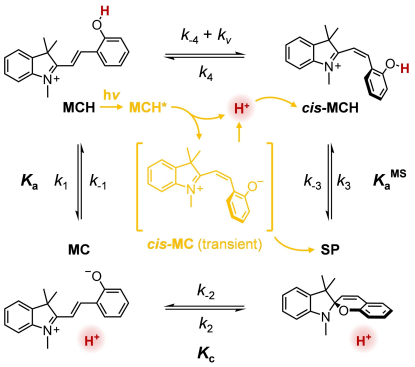

*C. Berton, Dr. C. Pezzato**

1 – 12

Photoacidity of Indolinospirobenzopyrans in Water